

Lawrence Berkeley National Laboratory

Recent Work

Title

RADIATION EFFECTS ON OPTICAL DATA TRANSMISSION SYSTEMS

Permalink

<https://escholarship.org/uc/item/2v15x89q>

Author

Leskovar, B.

Publication Date

1988-04-01

ca



Lawrence Berkeley Laboratory

UNIVERSITY OF CALIFORNIA

RECEIVED

LAWRENCE
BERKELEY LABORATORY

Engineering Division

MAR 3 1989

LIBRARY AND
DOCUMENTS SECTION

Presented at the IEEE 1988 Nuclear Science Symposium,
Orlando, FL, November 9-11, 1988, and to be published
in IEEE Transactions on Nuclear Science

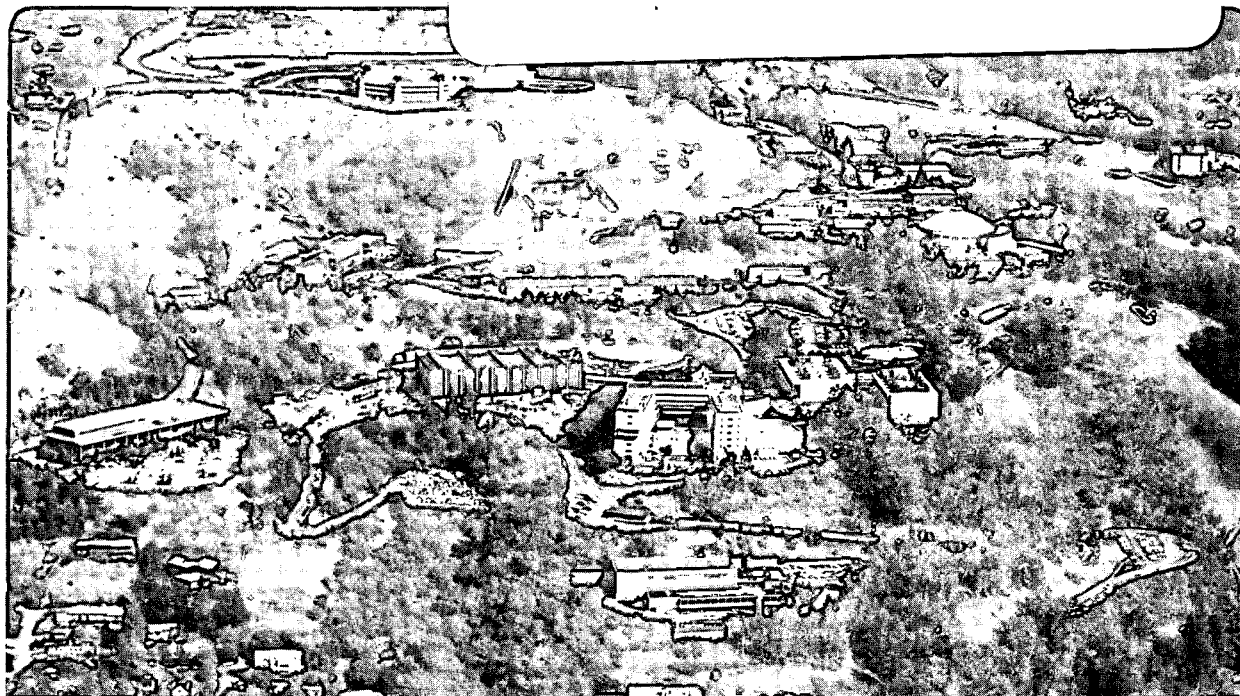
Radiation Effects on Optical Data Transmission Systems

B. Leskovar

April 1988

TWO-WEEK LOAN COPY

*This is a Library Circulating Copy
which may be borrowed for two weeks.*



LBL-25062
ca

DISCLAIMER

This document was prepared as an account of work sponsored by the United States Government. While this document is believed to contain correct information, neither the United States Government nor any agency thereof, nor the Regents of the University of California, nor any of their employees, makes any warranty, express or implied, or assumes any legal responsibility for the accuracy, completeness, or usefulness of any information, apparatus, product, or process disclosed, or represents that its use would not infringe privately owned rights. Reference herein to any specific commercial product, process, or service by its trade name, trademark, manufacturer, or otherwise, does not necessarily constitute or imply its endorsement, recommendation, or favoring by the United States Government or any agency thereof, or the Regents of the University of California. The views and opinions of authors expressed herein do not necessarily state or reflect those of the United States Government or any agency thereof or the Regents of the University of California.

Radiation Effects on Optical Data Transmission Systems

Branko Leskovar

Engineering Division
Lawrence Berkeley Laboratory
1 Cyclotron Road
Berkeley, California 94720

April 1988

Branko Leskovar

Lawrence Berkeley Laboratory
University of California
Berkeley, CA 94720 U.S.A.ABSTRACT

The state of the art of optical transmitters, low loss fiber waveguides and receivers in both steady state and pulsed radiation environments is reviewed and summarized. Emphasis is placed on the effects of irradiation on the performance of light emitting and laser diodes, optical fiber waveguides and photodiodes. The influence of radiation-induced attenuation of optical fibers due to total dose, dose rate, time after irradiation, temperature, radiation history, photobleaching, OH and impurity content, dopant type and concentration is described. The performance of candidate components of the transmission system intended for deployment in the Superconducting Super Collider Detector and primary beam tunnel nuclear environment is discussed.

INTRODUCTION

The Superconducting Super Collider Detector System will contain calorimetry, particle tracking, electron and muon identification subsystems, each involving typically 100,000 to 200,000 channels of readout electronics.

The overall detector system should be capable of operating with luminosity corresponding to an interaction rate of the order of 10^8 events per second. The required dynamic range is determined by the maximum energy that must be measured without saturation and by the precision that is required at low energy. Typically, the dynamic range will be of the order of 8 bits for the particle tracking chamber and 14 bits for the calorimeter subsystems.^{1,2} Furthermore, the nonlinearity should be less than 1% over the operating range for some subsystems. The high interaction rate, requires adequate time response capability of the readout electronics. In addition to wide dynamic range and fast time response, the readout electronics should have a power dissipation as low as possible, typically less than 50 mW/channel. This would make it possible to locate the entire front end readout electronics directly on or very close to the detector elements thus preserving the hermeticity of the calorimetry.

In general, for the SSC Detector System, if the signal transmission from the detector elements to the remote signal processing electronics and data acquisition subsystems were done by conventional cables it would present an extremely difficult packaging problem and would require an enormous space allocation. This in turn would compromise performance because of electromagnetic interference and signal loss as well as reduced maintainability and reliability of the complete detection system. To reduce the cable subsystem size and to simplify the overall system architecture it will be necessary to multiplex readout electronics using analog and digital fiber optics transmission links and radiation-hardened components.³⁻⁷ Furthermore, because the cost of electronics subsystems for SSC detectors will be a major part of the cost of the total detector system, the application of multiplexing and analog and digital fiber optics

transmission links in front end electronics, triggering and data acquisition will significantly reduce this cost.

An example of the use of fiber optic transmission links is given in Fig. 1 where signals are multiplexed onto the fiber optic waveguide after the Level I Trigger.⁷ Only sparse data are digitized from all the signals emanating from the detector and stored in the buffer memory. After the Level I Trigger has selected the potential events of interest, the data are passed on to the time division multiplexer. The time division multiplexer converts the data from parallel bits to serial bit form for transmission over fiber optic waveguide. After reception of the optical signals, the demultiplexer converts the serial signals back to parallel bits for storage in another buffer memory. The data are then passed through the Level II Trigger, the Software Trigger and on to the Processor Farm.

Another application of fiber optic transmission links is with the use of highly segmented detector subsystems in SSC detectors which require a large number of signal channels even with innovative schemes for sparse data scan logic. For example, high resolution pixel devices might be used for vertex detector which would require many signal channels to be read out from deep within the SSC detector. Highly multiplexed signal channels onto just a few high-speed fiber optic systems could be employed here. Multiplexing would alleviate the problem of the large number of wires which would otherwise be required for parallel dataways operating at tens of Mbit/s speeds.

Thus, the hermeticity of SSC detectors will be significantly improved by the use of fiber optic because of their lower space requirements as indicated in the above examples. Furthermore, the immunity to noise pickup and the low mass of fiber optic cables are additional advantages.

Similarly, an application of optical fibers appears attractive for a number of data transmission and communication tasks in various SSC accelerator systems.

The data base for the collider beam monitoring subsystems and control system must accommodate approximately 62,000 monitoring and control points.³ Each of these points has a number of words in the data base for its description and specification of properties. Monitoring and control points in the data base are divided among the various control subsystems. The control system of the collider consists of a host computer cluster, eight sector computers, two cluster computers, five injector subsystem computers, and approximately 400 distributed front-end processors. These computers and processors are connected together by local networks and a major long haul network of approximately 80 km in length. All the necessary communications from the central control facility to subsystems around the main accelerator ring will be accomplished by a ring information network using

broad band coaxial cables or optical fiber links. However, analog and digital transmission links and associated electronics components which will be used in the SSC detector and primary beam tunnel will be required to withstand exposure to the nuclear radiation background. Presently preliminary existing radiation background estimates for the dose rate and neutron fluence are 10^2 - 5×10^6 Gy/year and 10^{12} - 10^{13} n/cm²/year, respectively. These values of background radiation are high enough to cause an increase of optical losses of several orders of magnitude from the intrinsic fiber loss in some fibers. Also, optical losses can be very long-lived in some fibers, depending upon the glass or polymer composition.

This paper reviews the recent progress in understanding the behavior of optical fiber waveguides when they are exposed to ionizing and neutron radiation, and in explaining the defect centers giving rise to the radiation induced optical attenuation. Furthermore, a short review of radiation damage in associated electronics components and subassemblies, such as light emitting diodes, injection lasers, and optical receivers will be given.

OPTICAL SOURCES IN RADIATION ENVIRONMENT

Light emitting diodes and semiconductor lasers are the most frequently employed as light sources in optical systems.⁴⁻⁶ Light emitting diodes offer the advantages of simple fabrication and operation as well as low cost, high reliability and good linearity and small temperature dependence of the light output. Semiconductor index-guided injection laser diodes offer high output power level, efficiency and bit rate modulation capability as well as extremely narrow spectra and excellent mode stability of the emitted light.

The physical mechanism which causes radiation-induced degradation of the light output from LEDs is that nonradiative recombination centers are introduced which compete with radiative centers for excess carriers.⁸⁻⁹ This results in a decrease in minority carrier lifetime. These various centers, such as unintentionally added impurities, dislocations, growth-induced lattice defects and radiation induced lattice defects can act as sites for non-radiative recombination events producing heat. If lattice defects are introduced by exposure to a radiation dose or fluence Φ , the ratio of the preirradiation (L_0) and postirradiation (L) light outputs is given by

$$\left(\frac{L}{L_0}\right)^n = \frac{\tau_0}{\tau} = 1 + \tau_0 K \Phi \quad (1)$$

Where τ_0 and τ are total preirradiation and post irradiation lifetimes, respectively; K is damage constant which is determined by the physics governing the interaction of radiation with semiconductor material. The exponent $n = 1$, for a device with constant voltage operation where radiative current is diffusion controlled, $n = 2/3$ for a device constant current operation where L and current density are diffusion controlled and $n = 1/3$ for a device under constant current operation where L is diffusion controlled and current density is dominated by space charge recombination.

The damage constant is defined by

$$K \approx \sigma_{NR} v_{th} C \quad (2)$$

Where σ_{NR} is the carrier capture cross section associated with nonradiative centers, v_{th} is the minority carrier thermal velocity and C is the constant which magnitude depends on the probability of generation of a particular defects by a unit of radiation fluence.

When value of the term $\tau_0 \Phi$ is much larger than 1 the minority carrier lifetime will decrease leading to a corresponding decrease in the output light intensity (due to the increased strength of the non-radiative recombination). Studies have indicated that the radiation hardness of a device can be significantly increased by decreasing the product $\tau_0 K$. This can be accomplished by a heavy doping of the emitting region of the device and by operating the LED at high current densities.

Irradiation test performed on InGaAsP LEDs, with γ -rays operating at 1300 nm¹⁰, showed that no significant degradation of parameters can be observed up to a total dose of 10^5 Gy. The light output power decreased by 5% from the initial value upon an irradiation dose of 10^6 Gy. It was also estimated, that the light output power decreases to 50% of the initial value for the total dose of 2×10^7 Gy.

The normalized light output characteristics as a function of the neutron fluence for various LEDs under constant current operating conditions are shown in Fig. 2. The data are shown for the following devices: Plessey InGaAsP-High Radiance LED, Laser Diodes Laboratories GaAlAs IRE-160-High Radiance LED, Texas Instruments GaAlAs LED, Radio Corporation of America InGaAs LED, Hewlett Packard GaAs 4120 LED, and Texas Instrument GaAs: Si, Si LED. The high radiance (HR) devices, show the smallest sensitivity on the radiation. These LEDs have very small source and junction areas, so that the injected minority carrier current density is large even at moderate current levels. Consequently, it can be expected that the radiative recombination rate is enhanced at typical operating conditions. These devices can provide sufficient light output in many applications after neutron fluences in excess of 2×10^{14} n/cm².

Devices with GaAs:Si, Si junction are significantly more sensitive on radiation. The minority carrier lifetime in these LEDs is very long, typically 200-400 ns. Consequently the product $\tau_0 K$ is large, resulting in the output light decrease for approximately 10^3 when compared with typical GaAlAs LEDs at neutron fluence of 10^{14} n/cm², Fig. 2. The GaAs:Si, Si devices were originally developed for high initial light output.

Proton irradiation effects on the performance of variety of LEDs have been extensively studied.⁸ In Fig. 3 the light output characteristics as a function of diode current and 16-MeV proton and neutron fluence as parameters are shown. Measurements were made on Laser Diode Laboratory GaAlAs IRE-160-high radiance LED, emitting at 860 nm. A study of the characteristics reveals that the degradation rate is smaller at larger currents. Furthermore, comparison of the degradation rates, at large currents, indicates that 16-MeV protons are approximately 26 times more effective than neutrons in producing degradation in this device, because of value of $\tau_0 K$ is significantly larger for protons than for neutrons.

More recent studies of the effect of neutron irradiation on LEDs fabricated from strained-layer superlattice structures in the GaAs/GaAsP configuration show that there is no light output degradation

until a fluence of approximately $3 \times 10^{14} \text{ n/cm}^2$ is exceeded.⁹

Radiation induced degradation of the light output from the semiconductor laser diode is caused by a reduction of minority carrier lifetime resulting from displacement damage. Total light output of a GaAs laser diode as a function of current density with neutron fluence as a parameter is shown in Fig. 4. In the subthreshold region 1 of the characteristics, the laser behaves like a light emitting diode. The light output, at constant current, decreases with neutron fluence at about the same rate as for LEDs. At the beginning of lasing action (region 2) the neutron irradiation causes a strong decrease of light output. Finally, when the device is deeply in the lasing action (region 3), irradiation does not have a significant effect until the increase in the threshold current density prevents the laser from reaching region 3. Minority carrier lifetimes are of order 1 to 10 ps in GaAs junctions under intense stimulated emission. The lifetimes are of order 1-10 ns in sub-threshold region. Therefore, a much larger concentration of radiation induced defects is required to influence the radiative recombination rate in lasing region. Consequently, for radiation environment a semiconductor laser diode should be selected with a low threshold current and a very high maximum operating current. Recently developed double heterostructure GaAs laser diode has shown that it is still capable for lasing action after a neutron fluence in excess of $2 \times 10^{14} \text{ n/cm}^2$.

RADIATION-INDUCED ATTENUATION OF OPTICAL FIBERS

The optical properties of fiber waveguide are degraded by exposure to nuclear radiation, primarily through the generation of color centers in the fiber core. Color centers are formed by radiolytic electrons and holes which are trapped on defects that either exist in fiber prior to irradiation or are created by the exposure. These centers cause the optical attenuation which can be significantly greater than intrinsic fiber loss. In addition to the radiation-induced absorption light is generated in fibers during pulsed irradiation by photoexcitation of the color centers or by the Cerenkov process.

Radiation-induced attenuation consists of a permanent and metastable components. The permanent component lasts for a long period of time after initial exposure. The metastable component consists of transient part which decays by 10 dB/km in less 1 s after pulse irradiation and component which decays after 10 s after irradiation. The detailed behavior of the induced absorption depends on a number of factors such as the fiber parameters (fiber structure, core and cladding composition fabrication and dopants), radiation parameters (total dose, dose rate, time after irradiation, and energy, nature and history of the radiation), and system parameters (operational wavelength, light intensity and temperature).

The radiation-induced attenuation of fiber initially increases linearly with increasing dose under steady state irradiation as it is shown in Fig. 5. However, at higher doses, the loss characteristic shows saturation due to the recovery processes that occur simultaneously with the fiber darkening. The level of saturation depends upon fiber, radiation and system parameters. In multimode polymer clad silica fibers, having the high OH content core, such as Suprasil,¹¹ and manufactured in the late 1970's, saturation levels were near 70 dB/km at a total dose of 10^2 Gy and operating wavelength of 820 nm. At

doses higher than 10^2 Gy the induced loss decreased with increasing dose due to the radiation and photo-bleaching of color centers causing the absorption loss. Also, at doses larger than 10^4 Gy the fiber loss increased drastically because of embrittlement of the polymer. In multimode pure silica core fibers with fluorine doped cladding manufactured in the middle 1980's, saturation levels are near 5 dB/km at dose of 10^2 Gy.¹³

Because previous studies identified many variables that influence the radiation-induced effects in optical fibers, an international collaboration was organized to develop standardized testing procedures and assess the status of research and development relating to radiation response of optical fiber, fiber optics components and systems. Data shown in Figs. 5-11 and 13 are derived from information presented in Refs. 12 and 13.

Radiation induced attenuation and recovery characteristics for multimode Dainichi-Nippon St-100B fiber are shown in Figs. 5 and 6 using a LED injected optical power of $1 \mu\text{W}$ and a fiber length of 50 m. This fiber has a SiO_2 100 μm -diameter core, with a fluorine/boron doped SiO_2 140 μm -diameter cladding. The OH content and intrinsic attenuation is 5-10 ppm and 6.7 dB/km, respectively. The wavelengths of the injected optical signals were 840 and 850 nm. The fiber showed a radiation induced attenuation of 4.6 ± 0.27 dB/km at a 30 Gy total dose with a γ -rays dose rate of 3 Gy/min. The measured recovery with time of radiation-induced attenuation after exposure to 30 Gy is given in Fig. 6.

Also, the radiation-induced loss as a function of time for Dainichi-Nippon St-100B fiber exposed to pulsed irradiation with 5, 1.5×10^2 and 10^3 Gy dose is shown in Fig. 7. Similarly, in Fig. 8 the data are shown for the wavelengths of injected optical signals of 1280 and 1300 nm and power levels of $1 \mu\text{W}$ and $370 \mu\text{W}$. A comparison of the characteristics in Figs. 7 and 8 shows that significantly smaller initial induced attenuation are obtained at longer wavelengths.

The irradiation source was Hewlett Packard Febetron pulsed electron accelerator, Models 705 and 706, which provided 2 MeV electrons with 20-30 ns pulse width and 600 keV electrons width 2-3 ns pulse width, respectively. The wavelength of the injected optical signal was 840 nm at a power level of $600 \mu\text{W}$. The wavelength of the injected signal was 860 nm at optical power level of $1 \mu\text{W}$.

Radiation-induced loss characteristics for multimode Schott PH300 fiber exposed to pulsed irradiation of 10^3 Gy is shown in Fig. 9. This fiber has Fluosil SS 1.2 type preform, OH content of 800 ppm and preirradiation attenuation of 10 dB/km at a wavelength of 850 nm. The irradiation source was Hewlett-Packard Febetron pulsed electron accelerator, Models 705 and 706. The injected optical power levels were $0.2 \mu\text{W}$, $20 \mu\text{W}$ and $300 \mu\text{W}$. It can be seen from this figure that the recovery of the radiation induced attenuation is faster for higher amounts of injected optical power.

Influence of photobleaching on the radiation induced attenuation is shown in more details in Fig. 10. A multimode Schott P858E fiber having a length of 10 m was used for testing. This fiber was produced using plasma impulse chemical vapor deposition method. It has a SiO_2 104 μm -diameter core and fluorine doped SiO_2 254 μm -diameter cladding.

The OH content and preirradiation attenuation is 50 ppm and 3.6 db/km, respectively, at a wavelength of 850 nm. These measurements were performed using a dose rate of 3 Gy/min, and injected optical power levels of 0.1 μ W, 1 μ W and 10 μ W at the wavelength of 860 nm. It can be seen from Fig. 10 that there is a large dependence of the radiation-induced attenuation on the injected optical power level.

The radiation-induced attenuation can be also effectively decreased in optical fibers by radiation hardening. This attenuation as a function of wavelength, after a short 4 Gy exposure and radiation hardening dose of 0, 10^3 and 10^4 Gy, is shown in Fig. 11 for pure silica core fiber containing 150 ppm OH in the core.¹⁴ Preirradiation of the fiber resulted in added loss at short wavelengths but loss is smaller for wavelengths longer than 750 nm. Also, the effect of preirradiation can be seen in Fig. 12 for the Heraeus Fluosil SS 1.4 multimode fiber having SiO₂ 100 μ m-diameter core and fluorine doped 140 μ m-diameter cladding.¹³ This fiber has an OH content of 1500 ppm and preirradiation attenuation of 20 dB/km at wavelength of 850 nm. The second irradiation, 18 hours after the first, with dose rate of 3 Gy/min yielded a distinctly different course of the induced attenuation at lower doses. At larger doses, above 30 Gy, the attenuation for the first and second irradiation approaches asymptotically the same value. In these measurements the wavelength and injected optical power was 840 nm and 1 μ W, respectively.

The above discussion has centered on the behavior of multimode fiber waveguides in a radiation environment. Although bandwidths of approximately 2GHz X km can be obtained with this fiber, higher bandwidths require the use of single mode waveguides. The radiation response of single mode fibers is different from that of multimode waveguides because the larger part of optical power is transmitted through the cladding. Also, in single mode fibers the doping levels in core and cladding are smaller than those used for multimode fibers, because the required difference in the index of refraction is substantially smaller. Consequently, single mode fibers have demonstrated lower radiation sensitivity than multimode fibers.

Radiation-induced attenuation as a function of total dose and dose rate as parameter for a single mode Sumitomo fiber having a pure silica core and a fluorine doped cladding is shown in Fig. 13.^{15,16} This fiber was fabricated by the vapor axial deposition process. The fiber core diameter and cladding diameter is 8.5 μ m and 125 μ m, respectively. Depending upon the grade of the fiber, the preirradiation attenuation varies from 0.4 to 0.7 dB/km. Dispersion is smaller than 3.5 ps/nm/km for the range from 1285 to 1330 nm. Measurements were performed using ⁶⁰Co source and changing the dose rate from 1.0 to 10^3 Gy/hour. The injected optical power level was 20 nW at a wavelength of 1300 nm. It can be seen from Fig. 13 that the radiation-induced attenuation is 20 dB at total dose of 7×10^4 Gy and dose rate of 10^3 Gy/hour.

Similar measurements were performed on the fiber waveguide with the same geometry as given above but with germanium doped silica core and pure silica cladding. Under identical measuring conditions this fiber showed the radiation-induced attenuation of 20 dB at total dose of 1.5×10^4 Gy and dose rate of 10^2 Gy/hour.

Furthermore, both fiber waveguides were irradiated with 14 MeV neutrons. Results are shown in Fig.

15. The neutron induced attenuation of 20 dB was obtained after approximately 0.6 hour of irradiation for germanium doped core fiber. The attenuation increased up to 70 dB/km after 3.5 hours of irradiation (neutron fluence of 1.5×10^{14} n/cm²). However for pure silica core fiber the induced attenuation reached approximately 10 dB/km after the same irradiation time. Experimental results have clearly showed that pure silica core fiber has significantly lower radiation sensitivity than germanium doped silica core fiber for both γ -ray and neutron irradiation.

OPTICAL RECEIVER IN RADIATION ENVIRONMENT

High sensitivity optical receivers will be required for use in SSC networks particularly in high data rate long haul link. In radiation environment in which the optical data transmission systems will operate the optical detector of the receiver is found to be the limiting component. To achieve the required high performance the best possible detector and receiver configuration should be selected. An appraisal of the most prominent detector options for several Gbit/s data rates was summarized in Ref. 17.

The same physical process that make detectors sensitive for optical radiation also make most detectors sensitive to ionizing radiation. However, the ionizing radiation generates electron-hole pairs uniformly throughout the semiconductor material of the photodiode while optical radiation generates carriers only in the active region of the photodiode pn junction. Consequently low ionizing radiation sensitivity can be achieved by (1) reducing the volume of the active region and at the same time keeping the responsivity of the device to optical signals high, and (2) reducing the volume of the optically nonactive regions of the photodiode. Also, it is beneficial to reduce the collection at the photodiode junction of the ionization radiation-induced carriers from optically nonactive regions. The first task can be accomplished by fabricating the photodiode from III-V semiconductors, such as GaAs which have a large absorption coefficient at the wavelength of the optical radiation. In this case the photodiode active region is very thin, typically several tenths of a micron, offering a very small volume to ionizing radiation. The second task can be accomplished by a heterostructure configuration of the photodiode.⁹ In such configuration additional barrier layers are introduced and the geometry of the active region is precisely defined preventing collection of carriers from optically nonactive regions of the device.

Various radiation studies were performed on these radiation hardened devices, measuring an increase of leakage current caused by ionization and neutron irradiation.^{8,9} For comparison purposes a figure of merit was introduced, M_{pd} , defined as the ratio of the photodiode signal current per unit of incident optical flux to the ionization induced current per unit of dose rate. The figure of merit $M_{pd} = 40-70 \times 10^{-10}$ Gy/optical photon for a GaAs photodiode with heterostructure configuration. For comparison $M_{pd} = 0.5-2.0 \times 10^{-10}$ Gy/optical photon for a typical Si photodiode. This and other data have revealed that double heterostructure AlGaAs/GaAs devices are far superior to Si radiation hardened photodiodes. GaAs devices were able to operate up to 10^6 Gy/s, a level several orders of magnitude above the capability of Si PIN photodiodes.

It can be concluded from the measurements of neutron irradiation effects on photodiodes⁸ that the device leakage current increases by a factor of 10 in

the AlGaAs/GaAs photodiode and factor of 10^3 in the Si devices after exposure to a neutron fluence of $7 \times 10^{14} \text{ n/cm}^2$. At this neutron fluence there is no optical responsivity degradation of AlGaAs/GaAs photodiode while Si device responsivity decreased to 60% of its preirradiation level.

Similarly, in InGaAs photodiodes, intended for data transmission links with operating wavelengths of 1300 nm, no degradation of optical and electrical characteristics were observed up to 10^6 Gy dose, with an exception of leakage current. The leakage current increases up to a factor of 6 from the pre-irradiation value when the total radiation dose is 10^6 Gy.

CONCLUSIONS

From the above review it is apparent that optical sources, fiber waveguides and optical receivers suffer a measurable degradation of their operating characteristics when exposed to radiation. However, it is also apparent, that using existing radiation hardened components, and choosing an appropriate operating wavelength, analog and digital fiber optics transmission links can be designed to function during and immediately after exposure to ionizing radiation and neutron fluence expected in the SSC environment. Systems design will then include adequate optical power margins to maintain the signal-to-noise ratio necessary for reliable operation. It is essential to evaluate the expected incremental optical power loss in various SSC data transmission systems.

Accurate evaluation of the expected optical power loss in data transmission systems involves specific data on the amount and spatial distribution of the total dose, dose rate, required bandwidth and the environmental temperature in the SSC detector system and primary beam tunnel. The total dose and dose rate data are particularly important because the net radiation-induced attenuation in a fiber waveguide strongly depends on the competing processes of color center formation and recovery. In general, for smaller dose rate the induced attenuation is smaller, providing that the fiber recovers in the time scale of the exposure. Also, the attenuation can be significantly reduced by photobleaching effects, increasing the injected optical power levels and by higher environmental temperatures. Lower temperatures inhibit the recovery, thus causing greater attenuation by the steady state irradiation. In particular critical radiation environments the optical data link should be operated at longer wavelength, such as 1300 or 1500 nm, where the induced attenuation is smaller in comparison with that at shorter operating wavelengths.

However, it will be necessary to evaluate contemporary low radiation sensitivity fibers made by several manufacturers at long wavelengths for total doses larger than 10^2 Gy and dose rates typical for various SSC subsystems.

A choice between single mode or multimode fiber data link will primarily depend upon bandwidth requirements and allowable radiation sensitivity of each particular subsystem. For the SSC detector subsystem and primary beam local area networks the multimode fiber data link will suffice in most cases. For the long haul network the single mode fiber data link should be used. Because of the length of this network, which is approximately 80 km, a number of optical repeaters may be inserted in the data transmission links to recover optical power level of the signal if silica-based optical fiber are used.

The number of repeaters can be significantly reduced or completely eliminated if very long wavelength fluoride optical waveguides with low intrinsic attenuation and radiation sensitivity become available for deployment.

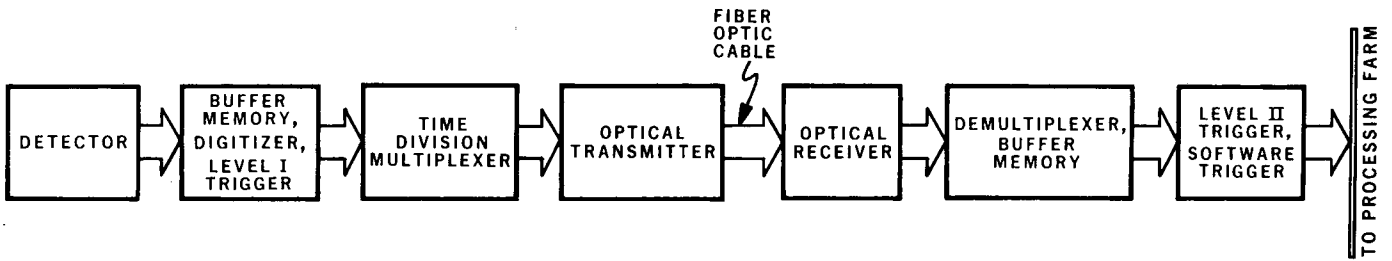
ACKNOWLEDGEMENTS

This work was performed as part of the program of the Electronics Research and Development Group, Electronics Engineering Department of the Lawrence Berkeley Laboratory, University of California, Berkeley. The work was partially supported by the U.S. Department of Energy under Contract Numbers DE-AC03-76SF00098. Reference to a company or product name does not imply approval or recommendation of the product by the University of California or the U.S. Department of Energy to the exclusion of others that may be suitable.

REFERENCES

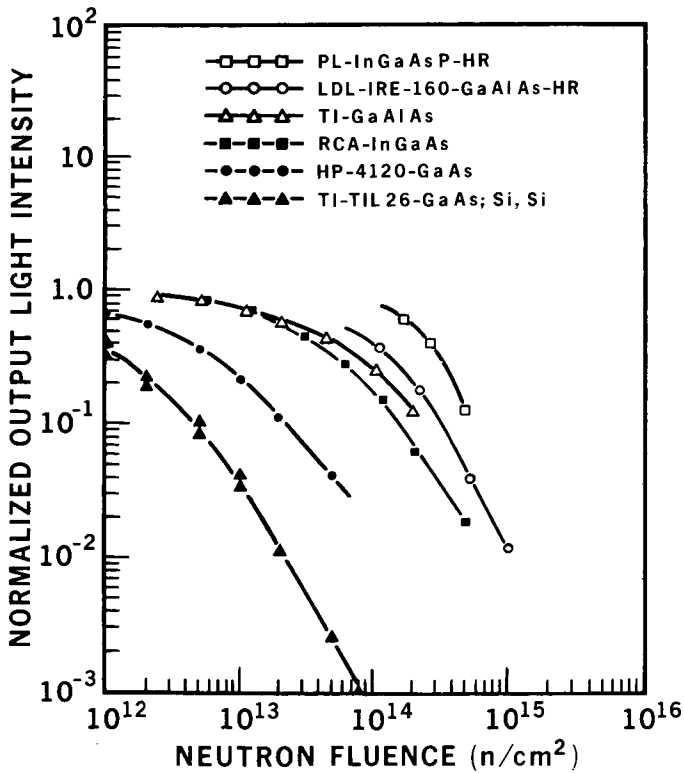
1. H.H. Williams, Detectors for the SSC: Summary Report, Proceedings of the 1986 Summer Study on the Physics of the Superconducting Supercollider, R. Donaldson and J. Marx, Eds., June 23-July 11, pp. 327-349, 1986.
2. T.J. Devlin, A. Lankford, and H.H. Williams, *ibid*, pp. 439-454.
3. SSC Central Design Group, Conceptual Design of the Superconducting Super Collider, SSC-SR-2020, March 1986.
4. B. Leskovar, M. Nakamura and B.T. Turko, Optical Wide Band Data Transmission System, Lawrence Berkeley Laboratory Report, LBL-23113, March 15, 1987.
5. B. Leskovar, M. Nakamura, and B.T. Turko, Wide Band Data Transmission System Using Optical Fibers, LBL-23304, April 23, 1987.
6. M. Nakamura, B. Leskovar, and B.T. Turko, Signal Processing in Wide Band Data Transmission System, LBL-23817, July 24, 1987.
7. B. Leskovar, M. Nakamura, F.A. Kirsten, and A.R. Clark, Study of Fiber Optics for Application to SSC Detector Systems, LBL PUB-5206, August 18, 1987.
8. B.H. Rose and C.E. Barnes, Proton Damage Effects on Light Emitting Diodes, *J. Appl. Phys.*, Vol. 53, No. 3, pp. 1772-1780, 1982.
9. C.E. Barnes, The Effects of Radiation on Optoelectronic Devices, Proceedings of SPIE-Fiber Optics in Adverse Environments III, Vol. 721, pp. 18-25, 1986.
10. H. Okuda, T. Fujitani et. al., Radiation Effects on InGaAsP/InP DH LEDs ($\lambda_p=1.3 \mu\text{m}$), 46th Meeting of the Japan Society of Applied Physics, 3a-N-1, p. 209, 1985.
11. E.J. Friebele, K.J. Long, C.G. Askins, M.E. Gingerich, M.J. Marrone and D.L. Griscom, Overview of Radiation Effects in Fiber Optics, Proceedings of SPIE - Radiation Effects in Optical Material, Vol. 541, pp. 70-88, 1985.

12. P.B. Lyons, NATO Radiation Effects Test Program for Optical Fibers and Components, Los Alamos National Laboratory Report LA-CP-87-200, 1987.
13. Report of the Nuclear Effects Task Group, NATO Panel IV, Research Study Group 12, P.B. Lyons (Ed.) Los Alamos National Laboratory Publication LA-CP-87-158, 1987.
14. R.H. West and A.P. Lenham, Radiation-Hardened Pure Silica-Core Fibre Optics, Electronics Letters, Vol. 19, No. 16, pp. 622-623, 1983.
15. Y. Chigusa, M. Watanabe, M. Kyoto, M. Oue, T. Matsubara, S. Okamoto, T. Yamamoto, T. Lida and K. Sumita, γ -Ray and Neutron Irradiation Characteristics of Pure Silica Core Single Mode Fiber and its Lifetime Estimation, Private Communication, T. Matsubara, January 1988.
16. T. Matsubara, M. Watanabe, H. Okuda, M. Taminoto, H. Kashiwara, Y. Fujita and N. Abe, Radiation Effects on Fiberoptic Signal Transmission Systems, Presented at the American Nuclear Society International Meeting, N.Y. September 14-18, 1986.
17. B. Leskovar, Optical Receivers for Wide Band Data Transmission System, Lawrence Berkeley Laboratory Report, LBL-25119, April 5, 1988.



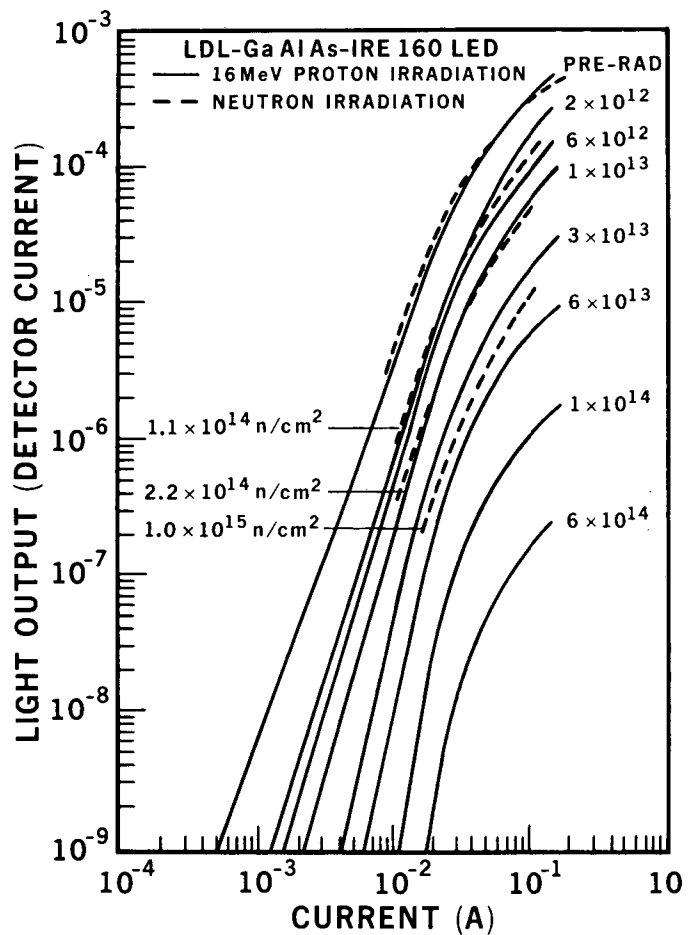
XBL 884-1171

Fig. 1. Simplified block diagram for fiber optic transmission link in SSC detector system.



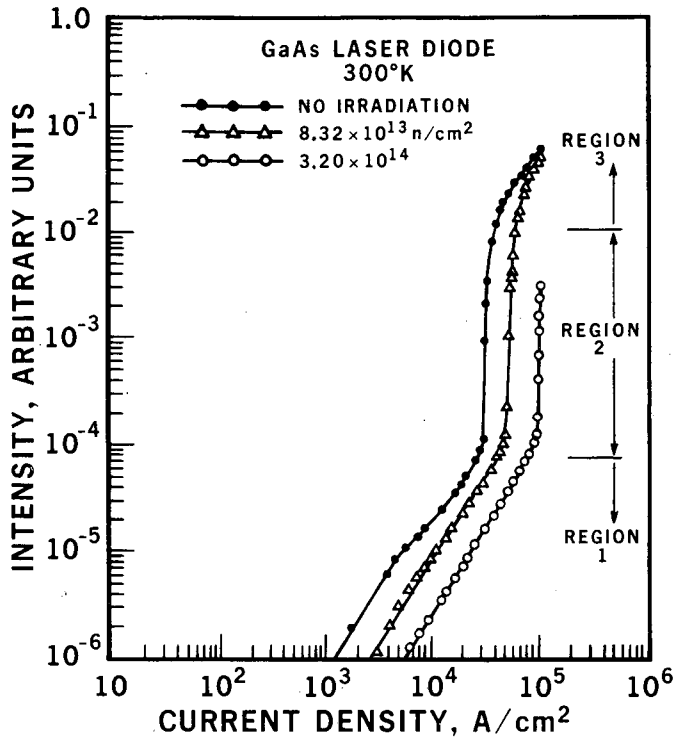
XBL 884-1172

Fig. 2. Normalized light output as a function of the neutron fluence for various LEDs under constant current operating conditions.



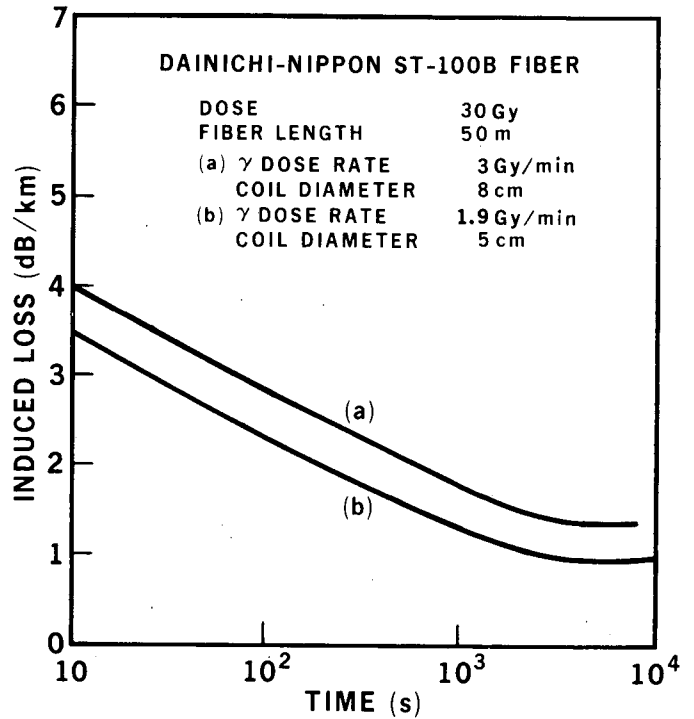
XBL 884-1173

Fig. 3. Light output as a function of LED current from a GaAlAs LED emitting at 820 nm with proton and neutron fluences as parameters.



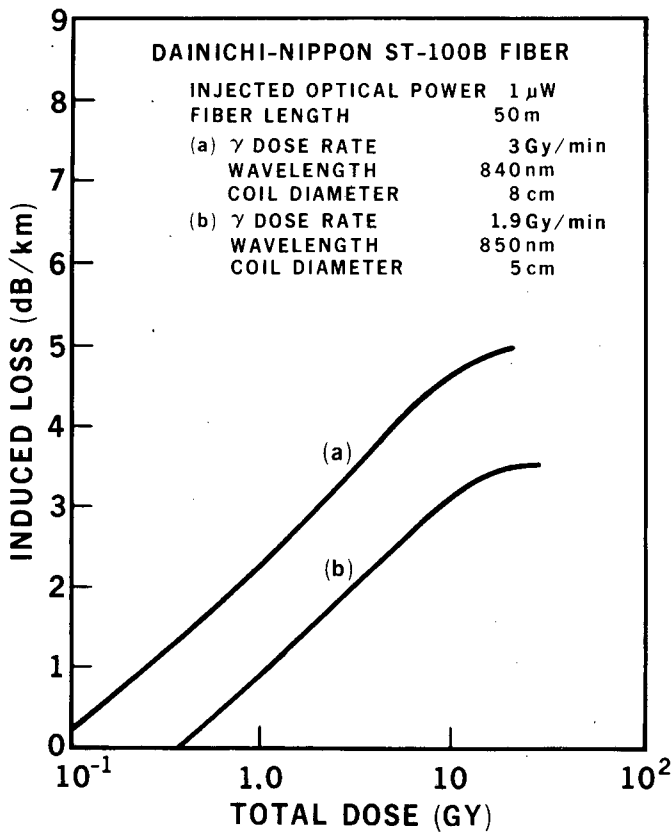
XBL 884-1174

Fig. 4. Light output a function of current density with neutron fluence as parameter for GaAs laser diode.



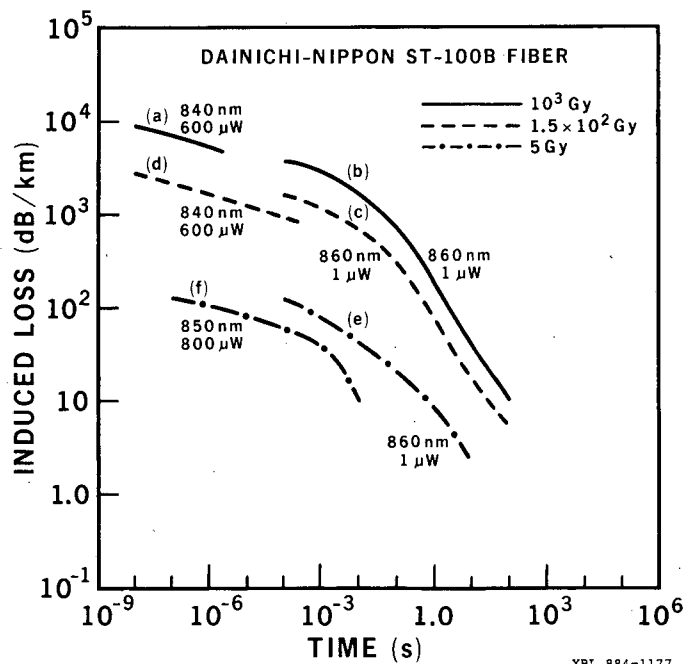
XBL 884-1176

Fig. 6. Recovery of radiation-induced attenuation for Dainichi-Nippon St-100B fiber after an irradiation to 30 Gy.



XBL 884-1175

Fig. 5. Radiation-induced attenuation in Dainichi-Nippon ST-100B fiber for 1.9 and 3 Gy/min γ dose rates.



XBL 884-1177

Fig. 7. Recovery of radiation-induced attenuation for Dainichi-Nippon ST-100B fiber after pulse irradiation exposure for wavelengths of 840-860 nm.

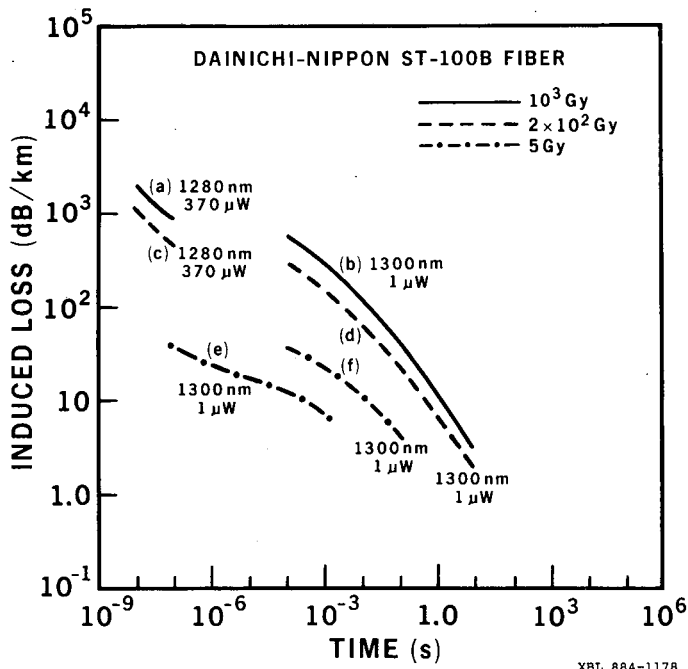


Fig. 8. Recovery of radiation-induced attenuation for Dainichi-Nippon ST-100B fiber after pulse irradiation exposure for wavelengths of 1280 and 1300 nm.

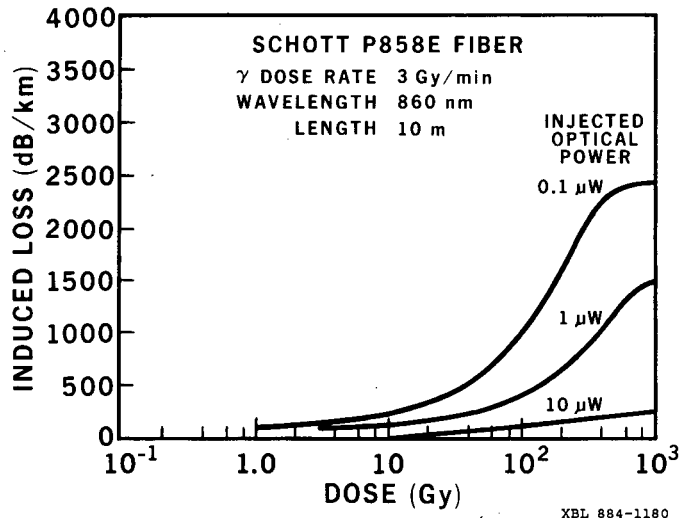


Fig. 10. Radiation-induced attenuation as a function of total dose with injected optical power level as parameter.

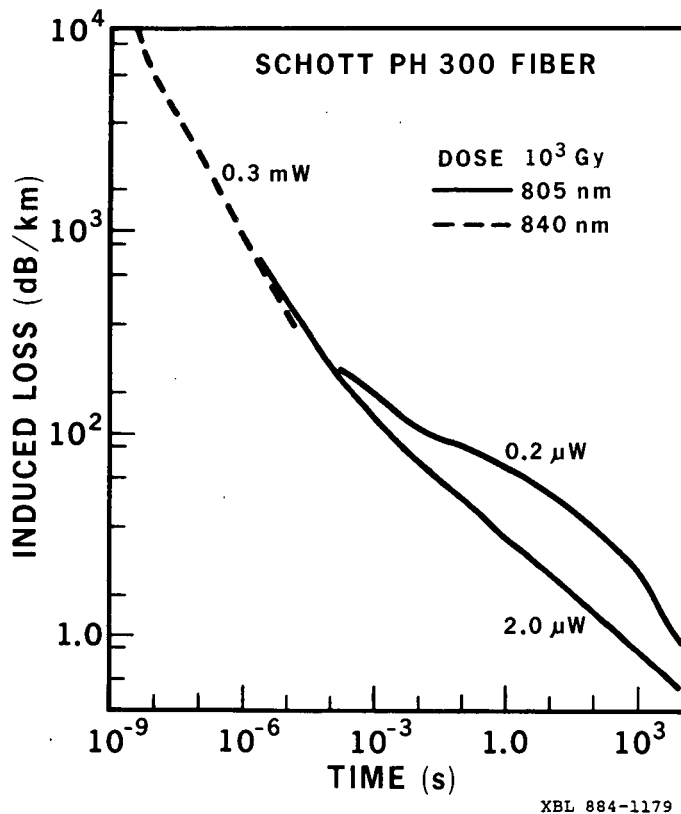


Fig. 9. Recovery of radiation-induced attenuation for Schott PH-300 fiber for wavelengths of 805 and 840 nm and injected optical power of 0.2 μ W, 2 μ W and 300 μ W.

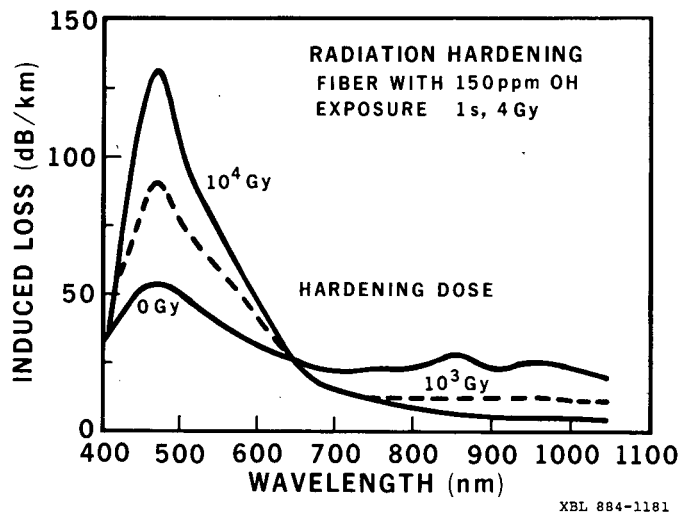


Fig. 11. Radiation-induced attenuation in a silica core fiber as a function of wavelength with hardening dose as a parameter.

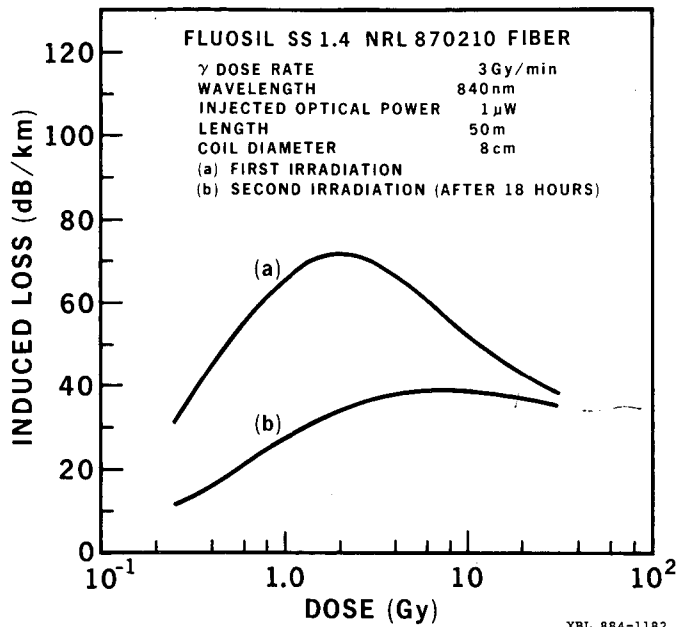


Fig. 12. Radiation-induced attenuation for Fluosil SS 1.4 fiber as a function of dose for the first and second irradiation.

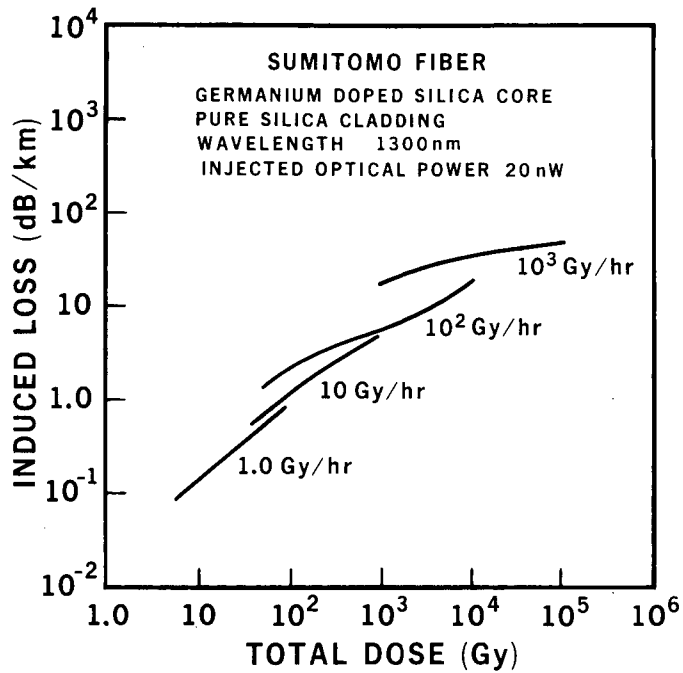


Fig. 14. Radiation-induced attenuation as a function of total dose with dose rate as parameter for single mode Sumitomo fiber having germanium doped silica core.

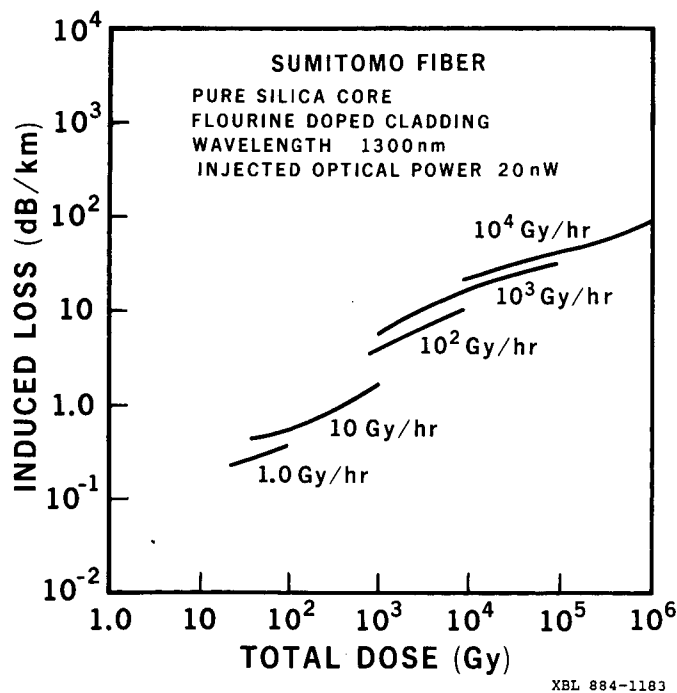


Fig. 13. Radiation-induced attenuation as a function of total dose with dose rate as parameter for single mode Sumitomo fiber having pure silica core.

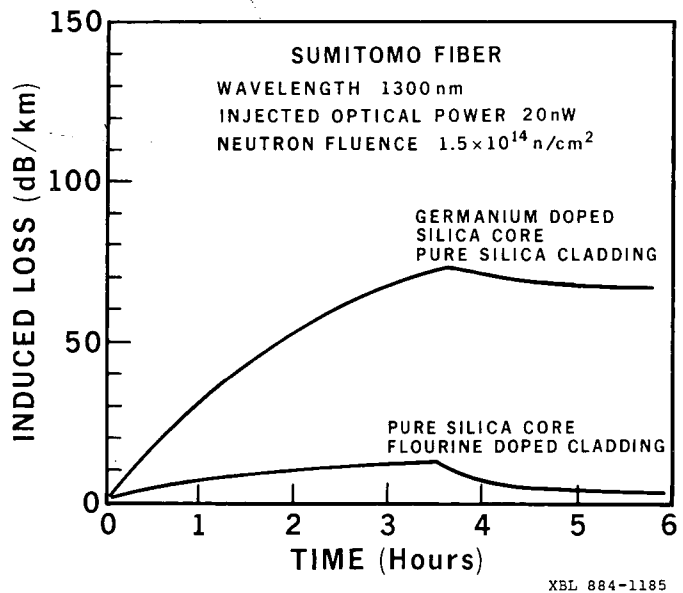


Fig. 15. Radiation-induced attenuation as a function of time for single mode Sumitomo fiber and 14 MeV neutron irradiation.

*LAWRENCE BERKELEY LABORATORY
TECHNICAL INFORMATION DEPARTMENT
UNIVERSITY OF CALIFORNIA
BERKELEY, CALIFORNIA 94720*